CHD4-NURD controls mouse neonate spermatogonia survival

Rodrigo O. de Castro[*], Victor Goitea[*], Luciana Previato[*], Agustin Carbajal[*], Courtney T. Griffin[†,‡], and Roberto J. Pezza[*,‡,§].

[*]Cell Cycle and Cancer Biology Research Program, Oklahoma Medical Research Foundation, Oklahoma City, Oklahoma, United States of America.

[†]Cardiovascular Biology Research Program, Oklahoma Medical Research Foundation, Oklahoma City, Oklahoma, United States of America.

[‡]Department of Cell Biology, University of Oklahoma Health Science Center, Oklahoma City, Oklahoma, United States of America.

[§]Corresponding author: Roberto J. Pezza. Suite B305. 825 NE 13th street, Oklahoma City, Oklahoma, 73104. Tel. 405-271-6467. Email: pezzar@omrf.org.

Running title: CHD4-NURD function in gametogenesis

Key words: mouse gametogenesis, spermatogonia, NURD, and testis development.

Abstract

Testis development and sustained germ cell production in adults rely on the establishment of spermatogonia stem cells and their proper differentiation into mature gametes. Control of these processes involves not only promoting the expression of genes required for cell survival and differentiation but also repressing other cell fates. This level of transcriptional control requires chromatin-remodeling complexes that restrict or promote transcription machinery. Here, we investigated the roles of the NUcleosome Remodeling and Deacetylase (NURD) complex during spermatogenesis. Our cellular and biochemical analyses revealed differential expression and composition of NURD subunits in germ cells at different stages of testis development. Germ cell-specific deletion of the NURD catalytic component Chd4, but not Chd3, resulted in arrested early gamete development due to failed cell survival of neonate undifferentiated spermatogonia stem cell population. Genome-wide chromatin localization suggested that CHD4 binds the promoters of genes involved in spermatogonia cell survival. Further genome-wide, cytological, and expression analysis revealed that CHD4 controls DMRT1 and its downstream target PLZF. DMRT1 and PLZF have been described as prominent regulators of spermatogonia stem cell maintenance. Together, our results uncover the requirements of CHD4 in mammalian gonad development and point to unique roles for the NURD complex with respect to other chromatin remodelers during gamete development.

Introduction

Defects in gametogenesis are a leading cause of infertility and an important cause of birth defects associated with aneuploidy. Insights into the mechanisms underlying testis formation, including spermatogonia stem cell and spermatocyte development, are necessary to improve the outcomes of common gonad developmental diseases.

In mice, spermatogenesis begins from isolated germ cells called spermatogonia A-singles (As) that undergo to a series of mitotic divisions to produce spermatogonia known as paired (Apr) and aligned (Aal) that contains chains of 4 to16 cells anchored by intercellular bridges as a result of with incomplete cytokinesis [1, 2]. At this point, spermatogonia cells start a process of differentiation (A1, A2, A3, A4 or intermediate (In)), formation of type B spermatogonia, and then transition to pre-leptotene cells that initiate the series of meiotic divisions that ultimately originate spermatozoa.

Chromatin undergoes extensive remodeling during gametogenesis, leading to altered gene expression and chromosome organization, and ultimately controlling obligatory developmental transitions such as the conversion from undifferentiated to differentiated spermatogonia type and spermatogonia commitment to meiosis [3, 4]. The NURD (NUcleosome Remodeling and Deacetylase) complex is a prominent chromatin modifying complex that functions to control gene expression via chromatin remodeling and histone deacetylation [5, 6]. The NURD complex contains two highly conserved and widely expressed catalytic subunits, CHD3/Mi-2α (chromodomain-helicase-DNA-binding 3) and CHD4/Mi-2β, which are members of the SNF2 superfamily of ATPases [5-9]. A third NURD member, CHD5, has also been described to function in the testis [10]. NURD plays a central role in various developmental and cellular events, such as controlling the differentiation of stem cells, maintaining cell identity, and responding to DNA damage [9, 11, 12]. In testis, CHD5 is required for normal spermiogenesis and proper spermatid chromatin condensation, while CHD3/4 has been described to localize at the X-Y pseudoautosomal region, the X centromeric region, and then spreads into the XY body chromatin [13]. Although the role of CHD5 has been well defined, no studies to date have addressed the requirements or mechanisms of CHD4 and CHD3 in any germ cell type.

In this study, we report that CHD4 (but not CHD3) is essential for testis development and sustained germ cell production. Germ cell-specific deletion of CHD4 results in the developmental arrest of undifferentiated spermatogonia in neonatal mice progressing to the Sertoli-only phenotype. Our system-wide studies of CHD4 target genes and subsequent cytological and expression analysis show that CHD4 binds at DMRT1 promoter and DMRT1 downstream targets such as PLZF. We propose this is the mechanism by which CHD4 contributes to early germ cell development by regulating genes that are required for survival/maintenance of spermatogonia cells. This study presents evidence of a mechanism in which CHD4 and the NURD complex regulate gamete development.

Results

Chd4 expression during mouse germ cell development

To investigate a potential role for CHD4 in germ cells, we assessed CHD4 expression in newborn and adult mouse testes by immunofluorescence. CHD4 was highly expressed in spermatogonia cells (marked by PLZF, aka ZBTB16) and in Sertoli cells (marked by SOX9) (Fig. 1A and Fig. S1), but not in the negative control (PLZF-positive spermatogonia from Ddx4-*Chd4*$^{-/-}$ testes, Fig. S2A). PLZF is expressed in undifferentiated spermatogonia [14]. The nuclear immunosignal of CHD4 is located mostly at the sex body pachytene cells (Fig. 1B). In agreement with a previous report [13], immunosignal of CHD4 was detected in late-pachytene stages associated to the pseudoautosomal region of the X-Y chromosomes (Fig. 1A, selected area on adult mouse top panel, and Fig. 1B). In sum, CHD4 is detected in spermatogonia, Sertoli cells, and primary spermatocytes.

We confirmed that CHD4 is expressed at both pre-meiotic and meiotic stages of male gamete development by analyzing CHD4 protein levels by western blot in enriched

fractions (see methods for details) of undifferentiated and differentiating spermatogonia (obtained from wild type 7dpp mice and using THY1.2+ and c-KIT+ affinity columns, respectively). CHD4 was also detected in the affinity column flow through (which was enriched in mostly Sertoli cells, here called Sertoli fraction), and pachytene spermatocytes (Fig. 1C). The level of cell population enrichment was assessed by western blot and markers specific for Sertoli (SOX9), undifferentiated spermatogonia (PLZF), differentiating spermatogonia (STRA8), and primary spermatocytes (SYCP3) (Fig. 1C). Our results are comparable to those published by Bergs, et. al. [13].

Composition of CHD4-NURD complexes during spermatogenesis

NURD function is influenced by its subunit composition [15, 16]. To determine whether the expression of NURD composition might change during spermatogenesis, first we analyzed the levels of representative NURD subunits in enriched fractions of undifferentiated and differentiating spermatogonia, Sertoli cells, and pachytene spermatocytes. Although NURD subunits HDAC2A, MTA1, RBBP4, RBBP7 and MBD2 were present in enriched fractions of undifferentiated (THY1.2+) and differentiating (c-KIT+) spermatogonia, the levels of MTA1, RBBP7, and MBD2 subunits were substantially reduced in pachytene spermatocytes (Fig. 1C), suggesting a particular composition and perhaps a different function for CHD4-NURD in this cell type.

To determine the composition of CHD4-NURD complexes, we used co-immunoprecipitation analysis to uncover NURD subunits that interact with CHD4 in enriched fractions of Sertoli and spermatogonia cells. The NURD subunits HDAC2A, MTA1, and RBBP4, but not MBD2, coimmunoprecipitated with CHD4 from Sertoli and Spermatogonia cells (Fig. 1D). HDAC2A coimmunoprecipitated with CHD4 from wild type and *Chd3*$^{-/-}$ spermatogonia cells (Fig. S2B). These data suggest that: i) CHD4 forms a NURD complex independently of CHD3, ii) CHD3 and CHD4 occupancy within the NURD

complex is mutually exclusive, and iii) that loss of CHD3 does not perturb CHD4-NURD complex formation in spermatogonia cells.

As expected, the CHD4 complexes we identified also include other components of the canonical NURD complex, HDAC2A, MTA1 and RBBP4/RBBP7.

Deletion of *Chd4* but not *Chd3* results in testis developmental defects

To examine the potential functions of *Chd4* and *Chd3* during spermatogenesis, we generated a series of *Chd4* and *Chd3* germline conditional knockout mice (Fig. 2A-D). To delete the floxed allele in gonocytes (embryonic day 15.5, Fig. 2C) [17], male Ddx4-Cre; $Chd4^{WT/\Delta}$ were crossed with $Chd4^{fl/fl}$ females to generate Ddx4-Cre; $Chd4^{fl/\Delta}$ conditional knockout mice (here called Ddx4-$Chd4^{-/-}$). A similar strategy was used to generate Ddx4-$Chd3^{-/-}$ mice (Fig. 2B), as well as Spo11-$Chd4^{-/-}$ mice, which delete the floxed allele only in early primary spermatocytes (Fig. 2C) [18]. We confirmed deletion of *Chd3* and *Chd4* by RT-qPCR (Fig. 2D) and immunolabeling of CHD4 (Fig. S2A).

Ddx4-$Chd4^{-/-}$ adult mice (2 months old) appeared normal in all aspects except in the reproductive tissues. Testes were significantly smaller in Ddx4-$Chd4^{-/-}$ males (mean: 0.017g ± SD: 0.005, number of quantified mice n=4 (8 testes), P≤0.0001, t test) compared to wild type (0.104 g ± 0.015, n=6 mice (12 testes)) littermates (Fig. 2E), indicating severe developmental defects in the testis. In contrast, Spo11-$Chd4^{-/-}$ (0.096g ± 0.011, number of quantified mice n=3 (6 testes); P=0.21, t test), and Ddx4-$Chd3^{-/-}$ males (0.095g ± 0.002, n=3 mice (6 testes), P=0.04, t test) did not show any significant difference in testis size compared to wild type littermates (Fig. 2E). Thus, CHD4, but not CHD3, plays an important role in mouse male gametogenesis. Moreover, the normal testis size of Spo11-$Chd4^{-/-}$ mice suggests that developmental defects triggered by CHD4 depletion originate in pre-meiotic stages of gamete development.

We found that adult Ddx4-*Chd4*$^{-/-}$ males develop testicular hypoplasia with hyperplasia of interstitial cells and lack spermatozoa (Fig. 3A). The number of seminiferous tubules is similar between wild type and mutant animals, but the diameter is reduced (wild type, mean ± SD, 287 ± 34, n=400 seminiferous tubules cross sections (3 different mice, 2-month-old) versus *Chd4*$^{-/-}$ 148 ± 21.3, n=210, P<0.0001 t test).

Analysis of Ddx4-*Chd4*$^{-/-}$ testes revealed a total loss of germ cells (marked by TRA98) in seminiferous tubules (Fig. 3B). No developing gametes were observed, including cell types at early stages (e.g., spermatogonia) (Fig. 3A and B). Sertoli cells develop normally in Ddx4-*Chd4*$^{-/-}$ mice, consistent with the specific loss of *Chd4* in germ cells at early stages of development. We did not observe differences in germ cell development between wild type and Ddx4-*Chd3*$^{-/-}$ or Spo11-*Chd4*$^{-/-}$ mice (Fig. S3A and B), consistent with their similar testis sizes (Fig. 2E).

We also analyzed H&E stained histological sections of ovaries from 45-day-old wild type and Ddx4-*Chd4*$^{-/-}$ female mice. We noted a significant reduction in ovary size, an increase in stromal cells, a reduced number of follicles (wild type, 10 ± 3, n=6 mice versus Ddx4-*Chd4*$^{-/-}$ 0.6 ± 0.9, n=5, P<0.0001 t test) and a reduced number of corpora lutea (wild type, 9 ± 1, n=6 mice versus Ddx4-*Chd4*$^{-/-}$ 0 ± 0, n=5, P<0.0001 t test) in the Ddx4-*Chd4*$^{-/-}$ mice compared to wild type (Fig. 3C).

We conclude that deletion of *Chd3* has apparent no effect on gamete development. However, germ cell specific deletion of *Chd4* results in severe male and female germ cell developmental defects, possibly originated at premeiotic stages of development.

Possible CHD4 function during mouse meiosis

CHD4 is known to play a role in the DNA damage response in somatic cells [6, 19, 20]. For example, *Chd4* knockdown results in increased γH2AX, a marker of double-strand breaks, and CHD4 accumulates at sites of DNA damage [4]. To determine whether CHD4

is required to repair the programmed double-strand breaks that occur in germ cells during meiosis, we immunostained spermatocyte chromosome spreads for γH2AX, a marker of DNA damage. In agreement with the normal development and cellular composition of Spo11-*Chd4*$^{-/-}$ testes (Fig. S3B), the kinetics of formation and repair of double-stand breaks appeared normal in Spo11-*Chd4*$^{-/-}$ mice (Fig. S4A, data was obtained from at least three mice of each phenotype). Further, chromosome pairing and synapsis in Spo11-*Chd4*$^{-/-}$ spermatocytes was indistinguishable from wild type cells.

Our results indicate that CHD4 has not an apparent role in progression of mouse meiosis. However, the lack of defective either DNA repair or homologous chromosome associations may be caused by the reduction, but not elimination, of CHD4 in Spo11-Chd4$^{-/-}$ mice (Fig. S4B and C).

CHD4 is required for neonate spermatogonia survival

The severe phenotypes observed in Ddx4-*Chd4*$^{-/-}$ mice (Fig. 2 and 3) prompted us to investigate spermatogonial differentiation during testis development in newborns. Testis sections from 9 dpp Ddx4-*Chd4*$^{-/-}$ mice stained with H&E showed a markedly reduced number of germ cells, as well as differences in cell composition, compared to those from age-matched wild type mice (Fig. 4A, a and b). To analyze this in detail, we examined the expression of TRA98 (a marker for germ cells) and STRA8, which marks differentiating spermatogonia and spermatocytes. Whereas tubules from 9 dpp wild type mice contained cells expressing TRA98 (45 ± 10, n=66 seminiferous tubules counted obtained from 3 mice) and STRA8 (18.8 ± 8.4, n=36 obtained from 3 mice), tubules from *Chd4*$^{-/-}$ mice showed a near absence of cells expressing these markers (TRA98, (4.6 ± 3, n=60 obtained from 3 mice, $P<0.0001$, Student t test). STRA8 2.5 ± 3.5, n=42 obtained from 3 mice, $P<0.0001$, Student t test) (Fig. 4A, c-f). Testes sections from 9 dpp *Chd4*$^{-/-}$ mice also showed a reduction in primary spermatocytes expressing the meiotic prophase I

markers SYCP3 and γH2AX compared to those from 9 dpp wild type mice (Fig. S5A and B). Together, the results further suggest that testis defects in *Chd4*$^{-/-}$ mice begin early, during pre-meiotic stages of postnatal development, leading to an absence of germ cells in adults. We note that in contrast to control, *Chd4*$^{-/-}$ knockout cells were mostly located at the periphery of the seminiferous tubules suggesting defects in germ cell migration and establishment of a proper cell niche (Fig. 4A).

To pinpoint when the testes defects originate in *Chd4*$^{-/-}$ mice, we stained testes sections from 1-21dpp mice for the expression of PLZF/ZBTB16 (undifferentiated neonate spermatogonia [14, 21]) and TRA98 (all germ cells). Compared to wild type, *Chd4* mutant sections displayed a small reduction in the number of cells expressing TRA98 at both 1dpp and 3dpp (Fig. 4B and 4C and Fig. S6). We observed equal numbers of SOX9-positive Sertoli cells in testes from wild type and *Chd4*$^{-/-}$ mice at 3, 4, and 9 dpp (Fig. 4C), as expected for the specific loss of *Chd4* in spermatogonia cells. Both PLZF-positive and TRA98-positive cells were substantially reduced in *Chd4*$^{-/-}$ mutant testis compared to wild type testis at 4 dpp and 7dpp (Fig. 4C).

Given that Chd4 may act as a regulator of cell-cycle progression, we then examined whether the rapid loss of PLZF-positive neonate spermatogonia in *Chd4*$^{-/-}$ testes was due to altered proliferative activity. We conducted EdU incorporation study to test this possibility. P4 mice were injected with EdU and analyzed 3 h later, after which we assayed its incorporation in PLZF-positive spermatogonia in whole mounts of seminiferous tubules (Fig. S7A). We found that spermatogonia cell proliferation (PLZF/EdU^{+} cells) in wild type and Ddx4-Chd4$^{-/-}$ is proportionally the same (Fig. S7C). In addition, reduced amount of total PLZF-positive cells was found in Ddx4-CHD4$^{-/-}$ compared to wild in the whole-mounting experiment (Fig. S7B).

To determine whether cell death contributed to the loss of Ddx4-*Chd4*$^{-/-}$ neonate spermatogonia (Fig. 4A-C), we performed TUNEL assay in staining paraffin embedded testis sections of wild type and *Chd4*$^{-/-}$ four days old testis. At this age the testis is mostly constituted by spermatogonia and Sertoli cells, which can be easily distinguished by DAPI nuclear staining patterns. We found a significantly increase of apoptotic cells in *Chd4*$^{-/-}$ testis compared to wild type mice (Fig. 4D).

We conclude that the possible cause of spermatogonia failure in *Chd4*$^{-/-}$ mice is in the survival/maintenance of neonate undifferentiated spermatogonia.

CHD4 binds the promoters of genes involved in neonate spermatogonia cell survival and differentiation

To investigate the mechanism of CHD4 requirement in neonate spermatogonia, we aimed to identify genes that are directly regulated by CHD4. We generated genome-wide chromatin-binding profiles of CHD4 in spermatogonia. We prepared enriched fractions of spermatogonia from 5 dpp wild type testes by magnetic-assisted cell separation (THY1.2+ and c-KIT+ cells) and analyzed CHD4 chromatin-binding analysis by chromatin immunoprecipitation combined with high-throughput sequencing (ChIP-seq) (Fig. 5). Heatmaps, aggregate profiles, and direct visualization of profiles revealed a prominent enrichment of CHD4 in promoter regions (Fig. 5A-D, Fig. S8 and table S1). Hierarchical clustering analysis around ± 3 Kb of gene bodies revealed two major types of CHD4 distribution (Fig. 5A). CHD4 binds to Cluster 1 genes throughout the gene body, with decreasing intensity from the transcription start site (TSS) (Figure 5A and B). In contrast, CHD4 binds to Cluster 2 genes exclusively at the TSS (Fig 5A-C, and table S2). We identified 2499 CHD4 peaks, distributed mainly in distal intergenic regions (41%), intronic regions (43%) and promoters (25%) (Fig. 5D). These regions often contain regulatory elements, suggesting that CHD4 regulates gene transcription in neonate spermatogonia.

To gain greater insight into the genes potentially regulated by CHD4, we annotated the peaks of CHD4 to the closest gene and performed functional analysis. Analysis of gene ontology (GO) initially revealed 469 terms associated with biological processes, 76 associated with molecular function, and 83 associated with cellular components (p. adjust <0.05) (table S3-5). The number of genes was reduced to 166, 40, and 30 terms, respectively, after consolidating related/similar terms. We observed approximately 50 genes involved in regulating chromosome organization, DNA repair, and the cell cycle (Fig. 5E and Fig. S8B). Interestingly, approximately 20 genes were involved in regulating stem cell survival and differentiation (Fig 5E and Fig. S8). We found Dmrt1, a known gene acting in spermatogonia cell maintenance/survival [22]. We also noted other genes that may be involved in regulating stem cell population maintenance/survival (Esco1, Pax2, and Vps72) and stem cell differentiation (Hes1, Rest, Tbx5, Sox5, and Setd1A), as their self may regulate transcription (e.g., acting as transcription factors) (Fig. 5F).

CHD4, DMRT1, and PLZF work together in a regulatory axis involved in spermatogonia cell survival

Prompted by the binding of CHD4 to the promoter region of the Dmrt1 gene (Fig. 6A), we tested Dmrt1 expression in Chd4 knockout versus wild type cells. We immunostained paraffined testes sections from 1, 4, and 7 dpp mice for the expression of DMRT1 (Fig. 6B and C). Compared to wild type, *Chd4* mutant showed a clear reduction in DMRT1 immunosignal. Then, to assess whether DMRT1 reduction was at the transcriptional level, we assayed RT-qPCR in Thy1+ enriched fractions of spermatogonia cells obtained from Chd4 knockout and wild type mice. As expected, we observed a substantial reduction in Dmrt1 transcript in Chd4 knockout compared to wild type cells (Fig. 6D), indicating that CHD4 may control Dmrt1 expression at the transcriptional level.

Recent work described that Dmrt1 controls Plzf expression, which is a transcription factor required for spermatogonia maintenance [22]. We then tested the effect of CHD4 depletion in Plzf expression. PLZF immunostaining of testes sections from 1, 4, and 7 dpp mice revealed a significantly reduction of this protein in Chd4 knockout cells respect to wild type. This is consistent with a model by which CHD4 control of Dmrt1 and downstream targets influences cell survival/maintenance.

We concluded that CHD4 participates in the maintenance/survival of neonate spermatogonia stem cell possibly through transcriptional regulation of genes participating in these critical processes.

Discussion

In this work, we examined the potential function of two critical NURD catalytic subunits, CHD4 and CHD3, in spermatogenesis. Our data suggest that a CHD4-NURD (but not CHD3-NURD) complex controls neonate spermatogonia development at early stages of testis development (Fig. 7). Germline deletion of *Chd4,* but not *Chd3,* results in a severe loss of germ cells specifically at early stages of the testis cord development. *Chd4* deletion affects spermatogonia, with the first obvious consequences in undifferentiated spermatogonia.

Most CHDs are expressed in testis; however, their insertion into the NURD complex seems to be developmentally regulated, with different patterns of expression during gametogenesis. CHD5 [7-9] has been shown to be expressed and required to compact chromatin in postmeiotic stages of spermatogenesis [10, 23]. In contrast, our results show that CHD4 is expressed and functions at premeiotic stages of

gametogenesis. We found that the composition of the NURD complex changes as spermatogenesis progresses, with loss of specific subunits in primary spermatocytes.

The functions of CHD4-NURD in neonate spermatogonia development and male gametogenesis are further revealed by our genome-wide analysis of CHD4 chromatin binding of enriched fractions of wild type mouse spermatogonia cells. We observed that CHD4 binds promoters of genes participating in cellular processes that support cellular survival/maintenance (Fig. 5 and 6). Among these genes we noted Dmrt1, which is a conserved transcriptional regulator with a role in mouse spermatogonia stem cell maintenance and replenishment [24]. Our subsequent cytological and transcriptional analysis confirmed that CHD4 regulate the expression of Dmrt1 (Fig. 6B-D). DMRT1 function in maintenance of spermatogonia stem cells has been proposed to be mediated by direct regulation of Plzf gene expression, another transcription factor required for spermatogonia maintenance [22]. In agreement with this possibility, we observed that the amount of PLZF was significantly reduced in Chd4 knockout versus wild type cells. In sum, our work provide evidence of a regulatory axis in which CHD4 may control important genes involved in spermatogonia stem cell maintenance and survival. Additional work will be required to test CHD4 effect in Sohlh1, another Dmrt1 direct target involved in cell survival and differentiation [22, 25, 26], and the Stra8 gene, the latter which precocious expression is detected in Dmrt1 knockout mice.

Chromatin remodeling complexes are a vast group of regulators with diverse functions in critical cellular processes such as transcription and DNA metabolism. They have been generally classified into four different families SWI/SNF, INO80, ISWI, and NURD. Most of the knowledge we have regarding their functions come from studies of somatic cultured cell models. More recently, however, work from different labs has begun exploring the role of chromatin remodelers in germ cell development. Germline-specific

deletion of *Brg1 or Brd7* [27-30] both components of the SWI/SNF complex, results in gonadal developmental defects. Deletion of *Ino80* in mouse spermatocyte resulted in a similar phenotype to that described for loss of SWI/SNF, with regard to meiotic prophase I failure in recombination and homologous chromosome associations [28, 31]. On the contrary, ISWI and CHD5 [32-34], the latter an alternative catalytic subunit of NURD complexes, function late in germ cell development with postmeiotic phenotypes associated with spermiogenesis and fertilization. Collectively, our studies show the unique cellular and molecular requirements of CHD4-NURD in early stages of gamete development. These results support a model in which distinct chromatin remodeling complexes fulfill specific requirements during different stages of gamete development.

Material and Methods

Mice

CHD4-floxed mice (*CHD4*$^{fl/fl}$) have been described [35]. *Chd3*-floxed mice were generated by Cyagen Biosciences using homologous recombination of a targeting vector in C57Bl/6 embryonic stem cells. The targeting vector incorporated a 5' LoxP site inserted between exons 12 and 13 and a 3' LoxP site inserted between exons 20 and 21 of the wild type *Chd3* allele. Transgenic *Cre* recombinase mice *Ddx4-Cre*$^{\text{FVB-Tg(Ddx4-cre)1Dcas/J}}$ was purchased from The Jackson Laboratory (Bar Harbor, ME). *Spo11*-Cre mice were kindly provided by Dr. P. Jordan (Johns Hopkins University Bloomberg School of Public Health, Baltimore, MD). *Chd3 or Chd4* gonad-specific knockouts and wild-type heterozygotes littermates were obtained from crosses between female homozygous *flox/flox* mice with male heterozygous Cre/+; *Chd3* Wt/flox and/or *Chd4* Wt/flox mice.

All experiments conformed to relevant regulatory standards guidelines and were approved by the Oklahoma Medical Research Foundation-IACUC (Institutional Animal Care and Use Committee).

Mice Genotyping

Characterization of wild type and *floxed* alleles was carried out by PCR using the following oligonucletides: CHD3 forward 5'-GGGTGGAGGTGGAAAGTGTA, CHD3 reverse 5'-AGAGGACAGGTCACAGGACAA, CHD4 forward 5'- TCCAGAAGAAGACGGCAGAT and CHD4 reverse 5'- CTGGTCATAGGGCAGGTCTC. The presence of *cre* recombinase allele were determine by PCR using the following primers: SPO11-Cre forward 5'-CCATCTGCCACCAGCCAG, SPO11-Cre reverse 5'-TCGCCATCTTCCAGCAGG, DDX4-Cre forward 5'-CACGTGCAGCCGTTTAAGCCGCGT, DDX4-Cre reverse 5'-TTCCCATTCTAAACAACACCCTGAA.

Real time-PCR

Total RNA was isolated from adult testis or from enriched fractions of spermatogonia with the Direct-zol RNA MiniPrep Plus kit (Zymo Research). RNA (2.0µg) was oligo-dT primed and reverse-transcribed with the high capacity RNA-to-cDNA kit (Applied Biosystems). Exon boundaries of *Chd4 and Chd3* were amplified using TaqMan Assays (Applied Biosystems) as directed by the manufacturer using Beta-2 macroglobulin as standard. TaqMan Mm01190896_m1 (Chd4), Mm01332658_m1 (Chd3), Mm00443809_m1 (Dmrt1), and Mm00437762_m1 (Beta-2 microglobulin). Gene expression was normalized with respect to wild type with wild type expression levels considered to be 1.

Western blot cell lysates

Total testis or enriched cells fractions were lysed in ice-cold protein extraction buffer containing 0.1% Nonidet P-40, 50 mM Tris-HCl, pH 7.9, 150 mM NaCl, 3 mM MgCl2, 3 mM EDTA, 10% glycerol, 1 mM DTT, 1mM PMSF and protease inhibitors (ThermoFisher Scientific, A32965) followed by sonication (3 pulses of 10 seconds) using micro ultrasonic cell disrupter (Kontes). The relative amount of protein was determined measuring absorbance at 260nm using NanoDrop 2000c spectrophotometer (ThermoFisher Scientific). Proteins were solubilized with 2X sample buffer (4% SDS, 160 mM Tris-HCl, pH 6.8, 20% glycerol, 4% mM β-mercaptoethanol, and 0.005% bromphenol blue) and 30 μg/lane of sample were separated by 4–15% gradient Tris-acetate SDS-PAGE and electro transferred to PVDF membrane (Santa Cruz Biotechnology, sc-3723). The blots were probed with individual primary antibodies, and then incubated with HRP-conjugated goat anti-mouse or rabbit antibody as required. In all blots, proteins were visualized by enhanced chemiluninescence and images acquired using Western Blot Imaging System c600 (Azure Biosystems). ImageJ software were used for quantification of non-saturated bands and α-tubulin were used for normalization. Antibodies used are detailed in table S6.

Histology and immunostaining

Testes and ovaries were dissected, fixed in 10% neutral-buffered formalin (Sigma) and processed for paraffin embedding. After sectioning (5–8-μm), tissues were positioned on microscope slides and analyzed using hematoxylin and eosin using standard protocols. For immunostaining analysis, tissue sections were deparaffinized, rehydrated and antigen was recovered in sodium citrate buffer (10 mM Sodium citrate, 0.05% Tween 20, pH 6.0) by heat/pressure-induced epitope retrieval. Incubations with primary antibodies were carried out for 12 h at 4°C in PBS/BSA 3%. Primary antibodies used in this study are detailed in table S6 Following three washes in 1 X PBS, slides were incubated for 1 h at

room temperature with secondary antibodies. A combination of fluorescein isothiocyanate (FITC)-conjugated goat anti-rabbit IgG (Jackson laboratories) with Rhodamine-conjugated goat anti-mouse IgG and Cy5-conjugated goat anti-human IgG each diluted 1：450 were used for simultaneous triple immunolabeling. Slides were subsequently counterstained for 3 min with 2μg/ml DAPI containing Vectashield mounting solution (Vector Laboratories) and sealed with nail varnish. We use Axiovision SE 64 (Carl Zeiss, inc.) for imaging acquisition and processing.

Primary spermatocyte enrichment

Synchronized pachytene spermatocytes from the first spermatogenic wave were purified as described in [36]. Briefly, 2 dpp mice were injected for seven consecutive days with WIN18,446 to arrest germ cells as spermatogonia. The next day (9 dpp), mice were injected with retinoic acid (RA) to induce their coordinated maturation. 2 Mice were killed at 13 days after RA injection (22 dpp). Testes were disaggregated using proteases and meiocytes were then purified by fluorescence activated cell sorting (FACS). Unlike Romer et al, after testes disaggregation and prior to FACS, cells were not washed (by centrifugation and resuspension) to avoid breakage of fragile pachytene cells. Instead, cells were sorted from the protease-containing buffer. Purity and stage of cells was assessed by immunofluorescence of chromosome spreads using anti SYCP1 and anti SYCP3 antibodies. More than 80% of cells were at pachytene stage.

Enrichment of Spermatogonia Populations

Our procedure of cell enrichment followed [37, 38]. Briefly, testis from 7dpp mice (or any other indicated age) were removed from mice and placed in a Petri dish containing Dulbecco's Modified Eagle Medium (DMEM without phenol red). After detachment of the

tunica albuginea, the seminiferous tubules were loosen using forceps and incubated in a 15 ml tube containing DMEM containing 1 mg/mL of collagenase, 300 U/mL of hyaluronidase and 5 mg/mL DNAse I (StemCell Technologies) under gentile agitation for 10 min. The seminiferous tubule clumps were pelleted by gravity and the cell suspension containing interstitial cells was discarded. The tubules were then incubated of with 0.05% Trypsin-EDTA solution (Mediatech Inc) for 5 min and the reaction was stopped by adding 10% volume of 10% BSA in PBS. Single cell suspension was obtained by mechanical resuspension followed by filtration through a 40-µm-pore-size cell strainer and dead cells were removed using Dead Cell Removal Kit (Miltenyi Biotec 130-090-101). Differentiating c-KIT+ neonate spermatogonia cells were magnetically labeled with CD117 (c-KIT+) MicroBeads (Miltenyi Biotec 130-091-224) and isolated using MS columns (Miltenyi Biotec 130-042-201) according to manufacturer's instructions. After the depletion of the c-KIT+ cells, the population of undifferentiated neonate spermatogonia cells were separated using CD90.2 (THY1.2+) MicroBeads (Miltenyi Biotec 130-121-278). Relative enrichment of cell populations was evaluated by STRA8 (c-Kit fractions) or PLZF (THY1.2 fractions) western blots (Fig. 1C). After c-kit and THY1.2 separation, the flow-through mostly contained Sertoli cells (SOX9 positive, Fig. 1C). The number of cells obtained from a pool of 4 mice testis at 7dpp was approximately 3.43×10^5 in THY1.2 fractions and 5.71×10^5 in c-Kit fractions.

Immunoprecipitation

Co-immunoprecipitation experiments were performed using testis of wild type or Ddx4-CHD3$^{-/-}$ mouse (Adult - 2 months old). After detunication, seminiferous tubules were loosen using forceps, washed twice with cold PBS and lysed using ice-cold RIPA buffer (50mM Tris pH 7.5, 150mM NaCl, 1% NP40, 0.5% Deoxycholate) containing protease inhibitors (ThermoFisher Scientific, A32965), sheared using 23G needle, incubated on ice

for 15 min and centrifugated at 1000xg for 10 minutes at 4ºC. Supernatant were collected in a separate tube, the pellet were resuspended in RIPA buffer, disrupted by sonication (3 pulses of 10 seconds) and centrifuged 12.000xg. This second supernatant was combined with the previous one and protein concentration was determined. We used 1mg of protein for each immunoprecipitation. Lysates were pre-cleared with protein G magnetic beads (BioRad, 161-4023) for 1 hour at room termperature and incubated with rabbit anti-CHD3 (5µg, Bethyl A301-220A), rabbit anti-CHD4 (2µg, Abcam ab72418), or rabbit IgG (5µg Jackson ImmunoResearch, 011-000-003). Lysates were rotated overnight at 4ºC and immune complexes were collected with protein G magnetic beads (2 hours at 4ºC). Beads were washed 4 times with washing buffer (50mM Tris pH 7.5, 150mM NaCl, 0.1% TX100, 5% glycerol) and two times with PBS. Proteins were eluted by boiling the beads with 2X sample buffer and analyzed by SDS-PAGE as described above.

EdU-based proliferation assay

Mice at indicated age received subcutaneous injection of EdU (50 mg/Kg) (Invitrogen, A10044) 3 hours prior euthanasia. After that, testes were removed and processed for whole-mount immunohistochemistry. EdU was detected by incubation of testis samples with reaction mix (2mM $CuSO_4$, 50 mM ascorbic acid and 2mM Alexa Azide conjugates (488 or 647) in PBS) for 3 hours at room temperature.

Whole-mount seminiferous tubules

Immunohistochemistry of whole-mount seminiferous tubules was performed as described [39]. Briefly, after detachment of the tunica albuginea, the seminiferous tubules were loosen using forceps and incubated in a 15 ml tube containing DMEM containing 1 mg/mL of collagenase, 300 U/mL of hyaluronidase and 5 mg/mL DNAse I (StemCell Technologies) under gentile agitation for 10 min. The seminiferous tubules clumps were

pelleted by gravity and the cell suspension containing interstitial cells was discarded. Seminiferous tubules were fixed for 4h in 4 % PFA (pH7.2 in PBS) at 4 ºC. After extensively wash in PBS, the tubules were permeabilized with series of MeOH/PBS (25, 50, 75, 95 %, and twice in 100 % MeOH) for 15 min at room temperature, treated with MeOH:DMSO:H_2O_2 (4:1:1), and rehydrated with MeOH/PBS (50, 25% and twice in PBS). Samples were incubated in ice-cold blocking solution PBSMT (PBS with 2% non-fat dry milk and 0.5% triton X-100) for 3 hours and then over-night at 4ºC with indicated primary antibodies under gentle rotation. Seminiferous tubules were washed in PBSMT (5 x 1h) and incubated with dye conjugated (Alexa488 or TRITC) goat anti-mouse or rabbit antibody as required. The tubules were mounted in raised coverslips glass slides.

Statistical Analyses

Results are presented as mean ± standard deviation (SD). Statistical analysis was performed using Prism Graph statistical software. Two-tailed unpaired Student's *t*-test was used for comparisons between 2 groups. $P < 0.05$ was considered statistically significant.

ChIP-seq

Undifferentiated and differentiating neonate spermatogonia cell fractions were obtained by affinity purification (C-KIT and THY1, respectively) of total wild type testis. ChIP was performed as previously described with modifications [40]. Mixed fractions of differentiating and undifferentiated cells were fixed for 5 min 1% methanol-free formaldehyde, quenched for 5 min with 125 mM glycine, and washed twice with PBS1X and resuspended in 5 mL of PBS1X containing 1mM of PMSF. Cells were broken by 20 strokes of douncing with a 'B' pestle, and then, pelleted at 2000 rpm for 5 min at 4°C. The cells were suspended in in 5 mL of Lysis buffer 1 containing 1mM PMSF (10 mM Tris-HCl

pH8, 10 mM EDTA, 0.5 mM EGTA, 0.25% Triton X-100) and centrifuged at 2000 rpm for 5 min at 4°C. The same procedure was repeated with 5mL of Lysis buffer 2 containing 1mM PMSF (10 mM Tris-HCl pH8, 1 mM EDTA, 0.5 mM EGTA, 200 mM NaCl). The cells were finally resuspended in 1 mL of ChIP buffer containing 1X protease inhibitor cocktail, Roche (50 mM Tris-HCl pH8, 1 mM EDTA, 150 mM NaCl, 1% Triton X-100, 0.1% Na deoxycholate, 0.1% SDS) and sonicated for 15 minutes using the Covaris E220 evolution. The sample was cleared at 12,000 g for 10 min at 4°C, and the chromatin was incubated with anti-CHD4 antibody (ab 70469, Abcam) overnight at 4°C. Antibody/chromatin complexes were captured with ChIP-grade protein A/G magnetic beads (ThermoFisher) for 2 h at 4°C and washed 2 times with increasing salt concentration (20 mM Tris-HCl pH8, 2 mM EDTA, 150-500 mM NaCl , 1% Triton X-100, 0.1% Na deoxycholate) and once with a Litium buffer (10 mM Tris-HCl pH8, 1 mM EDTA, 250 mM LiCl , 1% Igepal, 0.7% Na deoxycholate). The beads were washed twice with TE buffer pH7.4 (10 mM Tris-HCl, 1 mM EDTA) and DNA was eluted at 65°C with agitation for 30 minutes using 150 uL 1% SDS + 100 mM NaHCO3 made freshly (twice). Cross-links were reversed overnight by adding 5 uL of 5 M NaCl and incubating at 65°C. DNA was treated with 3 μL RNaseA (7000U/ml, Qiagen, 19101) for 30 min at 37° C and then 5 μl proteinase K (6000mAU/ml, Qiagen, 19131) for 1 h at 56° C. The DNA was purified using the miniElute PCR purification kit (Qiagen) and quantified using Qubit (Life Technologies) before library preparation (in-house or Kapa Hyperprep kit (KR0961)). Sequencing was performed on Illumina NextSeq 500 instrument in the OMRF Genomics core.

ChIP-seq data analysis

Quality metrics of the sequenced reads were computed using the tools FastQC (version 0.11.8), FastQ Screen (version 0.13.0) and AdapterRemoval (version 2.1.7) [36]. Pair end

75 bp reads from two independent experiments were aligned to mm10 using bwa (Version 0.7.17) [41, 42]. Picard (version 2.17.8) and SAMtools (version 1.9) were used to obtain mapping quality metrics, remove duplicates and filter unique reads [43, 44]. Only the uniquely aligned reads passing the quality filtering were selected for calculations reported here. MultiQC (version 1.7) was used to generate metrics reports [45]. The predominant insert-size (fragment length) based on strand cross-correlation peak was computed using phantompeaksqualtools (version 1.14) [46]. Bigwig coverage tracks were generated using bamCoverage tool from deepTools (version 3.1.3) [47, 48], with a binsize of 50 bp and extending fragments to 300bp and further smooth length 150 bp. Average profiles and heatmaps were plot using Deeptools (Peaks were called using MACS (version 2.1.2) [49, 50] using the broad mode and the following parameters: broad-cutoff 0.05, nomodel, extsize 200. In addition, we filter the peaks against the ENCODE blacklist regions and we further merged any peaks within 500 bp of the nearest peakusing bedtools (version 2.27.1) [51]. Peaks annotation and functional analysis was implemented in the R statistical software (www.R-project.org). Peaks were annotated for the nearest transcription start site using ChIPseeker package [52] and the annotation was based on org.Mm.eg.db mapping using Entrez Gene identifiers. Gene ontology analysis was done using clusterProfiler package [53]. The simplify function from clusterProfiler package with a cutoff of 0.7 was applied to remove redundant terms. Table S7 describes details of NGS datasets and analysis.

Acknowledgments. We thank Angela Andersen from Life Science Editors editorial services for her assistance in manuscript writing.

References

1. Greenbaum MP, Yan W, Wu MH, Lin YN, Agno JE, Sharma M, et al. TEX14 is essential for intercellular bridges and fertility in male mice. Proc Natl Acad Sci U S A. 2006;103(13):4982-7. Epub 2006/03/22. doi: 10.1073/pnas.0505123103. PubMed PMID: 16549803; PubMed Central PMCID: PMCPMC1458781.
2. Phillips BT, Gassei K, Orwig KE. Spermatogonial stem cell regulation and spermatogenesis. Philos Trans R Soc Lond B Biol Sci. 2010;365(1546):1663-78. doi: 10.1098/rstb.2010.0026. PubMed PMID: 20403877; PubMed Central PMCID: PMCPMC2871929.
3. Wang L, Xu Z, Khawar MB, Liu C, Li W. The histone codes for meiosis. Reproduction (Cambridge, England). 2017;154(3):R65-R79. doi: 10.1530/REP-17-0153. PubMed PMID: 28696245.
4. Stanley FK, Moore S, Goodarzi AA. CHD chromatin remodelling enzymes and the DNA damage response. Mutat Res. 2013;750(1-2):31-44. doi: 10.1016/j.mrfmmm.2013.07.008. PubMed PMID: 23954449.
5. Goodarzi AA, Kurka T, Jeggo PA. KAP-1 phosphorylation regulates CHD3 nucleosome remodeling during the DNA double-strand break response. Nat Struct Mol Biol. 2011;18(7):831-9. doi: 10.1038/nsmb.2077. PubMed PMID: 21642969.
6. Larsen DH, Poinsignon C, Gudjonsson T, Dinant C, Payne MR, Hari FJ, et al. The chromatin-remodeling factor CHD4 coordinates signaling and repair after DNA damage. J Cell Biol. 2010;190(5):731-40. doi: 10.1083/jcb.200912135. PubMed PMID: 20805324; PubMed Central PMCID: PMCPMC2935572.
7. Pan MR, Hsieh HJ, Dai H, Hung WC, Li K, Peng G, et al. Chromodomain helicase DNA-binding protein 4 (CHD4) regulates homologous recombination DNA repair, and its deficiency sensitizes cells to poly(ADP-ribose) polymerase (PARP) inhibitor treatment. J Biol Chem. 2012;287(9):6764-72. doi: 10.1074/jbc.M111.287037. PubMed PMID: 22219182; PubMed Central PMCID: PMCPMC3307306.
8. Polo SE, Kaidi A, Baskcomb L, Galanty Y, Jackson SP. Regulation of DNA-damage responses and cell-cycle progression by the chromatin remodelling factor CHD4. EMBO J. 2010;29(18):3130-9. doi: 10.1038/emboj.2010.188. PubMed PMID: 20693977; PubMed Central PMCID: PMCPMC2944064.
9. Clapier CR, Cairns BR. The biology of chromatin remodeling complexes. Annu Rev Biochem. 2009;78:273-304. doi: 10.1146/annurev.biochem.77.062706.153223. PubMed PMID: 19355820.
10. Zhuang T, Hess RA, Kolla V, Higashi M, Raabe TD, Brodeur GM. CHD5 is required for spermiogenesis and chromatin condensation. Mech Dev. 2014;131:35-46. doi: 10.1016/j.mod.2013.10.005. PubMed PMID: 24252660; PubMed Central PMCID: PMCPMC3965579.
11. Torchy MP, Hamiche A, Klaholz BP. Structure and function insights into the NuRD chromatin remodeling complex. Cell Mol Life Sci. 2015;72(13):2491-507. doi: 10.1007/s00018-015-1880-8. PubMed PMID: 25796366.
12. Eisen JA, Sweder KS, Hanawalt PC. Evolution of the SNF2 family of proteins: subfamilies with distinct sequences and functions. Nucleic Acids Res. 1995;23:2715-23.
13. Bergs JW, Neuendorff N, van der Heijden G, Wassenaar E, Rexin P, Elsasser HP, et al. Differential expression and sex chromosome association of CHD3/4 and CHD5 during spermatogenesis. PLoS ONE. 2014;9(5):e98203. Epub 2014/05/23. doi: 10.1371/journal.pone.0098203. PubMed PMID: 24849318; PubMed Central PMCID: PMCPMC4029951.
14. Costoya JA, Hobbs RM, Barna M, Cattoretti G, Manova K, Sukhwani M, et al. Essential role of Plzf in maintenance of spermatogonial stem cells. Nat Genet. 2004;36(6):653-9. Epub 2004/05/25. doi: 10.1038/ng1367. PubMed PMID: 15156143.

15. Margolin G, Khil PP, Kim J, Bellani MA, Camerini-Otero RD. Integrated transcriptome analysis of mouse spermatogenesis. BMC Genomics. 2014;15:39. doi: 10.1186/1471-2164-15-39. PubMed PMID: 24438502; PubMed Central PMCID: PMCPMC3906902.
16. Nitarska J, Smith JG, Sherlock WT, Hillege MM, Nott A, Barshop WD, et al. A Functional Switch of NuRD Chromatin Remodeling Complex Subunits Regulates Mouse Cortical Development. Cell reports. 2016;17(6):1683-98. doi: 10.1016/j.celrep.2016.10.022. PubMed PMID: 27806305; PubMed Central PMCID: PMCPMC5149529.
17. Gallardo T, Shirley L, John GB, Castrillon DH. Generation of a germ cell-specific mouse transgenic Cre line, Vasa-Cre. Genesis. 2007;45(6):413-7. Epub 2007/06/07. doi: 10.1002/dvg.20310. PubMed PMID: 17551945; PubMed Central PMCID: PMC2597027.
18. Pellegrini M, Claps G, Orlova VV, Barrios F, Dolci S, Geremia R, et al. Targeted JAM-C deletion in germ cells by Spo11-controlled Cre recombinase. J Cell Sci. 2011;124(Pt 1):91-9. doi: 10.1242/jcs.072959. PubMed PMID: 21147852; PubMed Central PMCID: PMC3001409.
19. Smeenk G, Wiegant WW, Vrolijk H, Solari AP, Pastink A, van Attikum H. The NuRD chromatin-remodeling complex regulates signaling and repair of DNA damage. J Cell Biol. 2010;190(5):741-9. doi: 10.1083/jcb.201001048. PubMed PMID: 20805320; PubMed Central PMCID: PMCPMC2935570.
20. Qi W, Chen H, Xiao T, Wang R, Li T, Han L, et al. Acetyltransferase p300 collaborates with chromodomain helicase DNA-binding protein 4 (CHD4) to facilitate DNA double-strand break repair. Mutagenesis. 2016;31(2):193-203. doi: 10.1093/mutage/gev075. PubMed PMID: 26546801.
21. Buaas FW, Kirsh AL, Sharma M, McLean DJ, Morris JL, Griswold MD, et al. Plzf is required in adult male germ cells for stem cell self-renewal. Nat Genet. 2004;36(6):647-52. Epub 2004/05/25. doi: 10.1038/ng1366. PubMed PMID: 15156142.
22. Zhang T, Oatley J, Bardwell VJ, Zarkower D. DMRT1 Is Required for Mouse Spermatogonial Stem Cell Maintenance and Replenishment. PLoS Genet. 2016;12(9):e1006293. Epub 2016/09/02. doi: 10.1371/journal.pgen.1006293. PubMed PMID: 27583450; PubMed Central PMCID: PMCPMC5008761.
23. Li W, Wu J, Kim SY, Zhao M, Hearn SA, Zhang MQ, et al. Chd5 orchestrates chromatin remodelling during sperm development. Nature communications. 2014;5:3812. doi: 10.1038/ncomms4812. PubMed PMID: 24818823; PubMed Central PMCID: PMCPMC4151132.
24. Wang F, Yu Y, Ji D, Li H. The DMRT gene family in amphioxus. J Biomol Struct Dyn. 2012;30(2):191-200. Epub 2012/06/19. doi: 10.1080/07391102.2012.677770. PubMed PMID: 22702730.
25. Matson CK, Murphy MW, Griswold MD, Yoshida S, Bardwell VJ, Zarkower D. The mammalian doublesex homolog DMRT1 is a transcriptional gatekeeper that controls the mitosis versus meiosis decision in male germ cells. Dev Cell. 2010;19(4):612-24. Epub 2010/10/19. doi: 10.1016/j.devcel.2010.09.010. PubMed PMID: 20951351; PubMed Central PMCID: PMCPMC2996490.
26. Suzuki H, Ahn HW, Chu T, Bowden W, Gassei K, Orwig K, et al. SOHLH1 and SOHLH2 coordinate spermatogonial differentiation. Dev Biol. 2012;361(2):301-12. Epub 2011/11/08. doi: 10.1016/j.ydbio.2011.10.027. PubMed PMID: 22056784; PubMed Central PMCID: PMCPMC3249242.
27. Yodh J. ATP-Dependent Chromatin Remodeling. Adv Exp Med Biol. 2013;767:263-95. doi: 10.1007/978-1-4614-5037-5_13. PubMed PMID: 23161016.
28. Kim Y, Fedoriw AM, Magnuson T. An essential role for a mammalian SWI/SNF chromatin-remodeling complex during male meiosis. Development. 2012;139(6):1133-40.

Epub 2012/02/10. doi: 10.1242/dev.073478. PubMed PMID: 22318225; PubMed Central PMCID: PMC3283123.
29. Wang J, Gu H, Lin H, Chi T. Essential roles of the chromatin remodeling factor BRG1 in spermatogenesis in mice. Biol Reprod. 2012;86(6):186. Epub 2012/04/13. doi: 10.1095/biolreprod.111.097097. PubMed PMID: 22495890; PubMed Central PMCID: PMCPMC3386149.
30. Wang H, Zhao R, Guo C, Jiang S, Yang J, Xu Y, et al. Knockout of BRD7 results in impaired spermatogenesis and male infertility. Scientific reports. 2016;6:21776. Epub 2016/02/18. doi: 10.1038/srep21776. PubMed PMID: 26878912; PubMed Central PMCID: PMCPMC4754950.
31. Serber DW, Runge JS, Menon DU, Magnuson T. The Mouse INO80 Chromatin-Remodeling Complex Is an Essential Meiotic Factor for Spermatogenesis. Biol Reprod. 2016;94(1):8. doi: 10.1095/biolreprod.115.135533. PubMed PMID: 26607718; PubMed Central PMCID: PMCPMC4809561.
32. Dowdle JA, Mehta M, Kass EM, Vuong BQ, Inagaki A, Egli D, et al. Mouse BAZ1A (ACF1) is dispensable for double-strand break repair but is essential for averting improper gene expression during spermatogenesis. PLoS Genet. 2013;9(11):e1003945. doi: 10.1371/journal.pgen.1003945. PubMed PMID: 24244200; PubMed Central PMCID: PMCPMC3820798.
33. Broering TJ, Wang YL, Pandey RN, Hegde RS, Wang SC, Namekawa SH. BAZ1B is dispensable for H2AX phosphorylation on Tyrosine 142 during spermatogenesis. Biol Open. 2015;4(7):873-84. doi: 10.1242/bio.011734. PubMed PMID: 25979708; PubMed Central PMCID: PMCPMC4571090.
34. Thompson PJ, Norton KA, Niri FH, Dawe CE, McDermid HE. CECR2 is involved in spermatogenesis and forms a complex with SNF2H in the testis. J Mol Biol. 2012;415(5):793-806. doi: 10.1016/j.jmb.2011.11.041. PubMed PMID: 22154806.
35. Williams CJ, Naito T, Arco PG, Seavitt JR, Cashman SM, De Souza B, et al. The chromatin remodeler Mi-2beta is required for CD4 expression and T cell development. Immunity. 2004;20(6):719-33. Epub 2004/06/11. doi: 10.1016/j.immuni.2004.05.005. PubMed PMID: 15189737.
36. Romer KA, de Rooij DG, Kojima ML, Page DC. Isolating mitotic and meiotic germ cells from male mice by developmental synchronization, staging, and sorting. Dev Biol. 2018;443(1):19-34. Epub 2018/08/28. doi: 10.1016/j.ydbio.2018.08.009. PubMed PMID: 30149006.
37. Oatley JM, Brinster RL. Spermatogonial stem cells. Methods Enzymol. 2006;419:259-82. Epub 2006/12/05. doi: 10.1016/S0076-6879(06)19011-4. PubMed PMID: 17141059.
38. Hammoud SS, Low DH, Yi C, Lee CL, Oatley JM, Payne CJ, et al. Transcription and imprinting dynamics in developing postnatal male germline stem cells. Genes Dev. 2015;29(21):2312-24. Epub 2015/11/08. doi: 10.1101/gad.261925.115. PubMed PMID: 26545815; PubMed Central PMCID: PMCPMC4647563.
39. Gassei K, Valli H, Orwig KE. Whole-mount immunohistochemistry to study spermatogonial stem cells and spermatogenic lineage development in mice, monkeys, and humans. Methods Mol Biol. 2014;1210:193-202. Epub 2014/09/01. doi: 10.1007/978-1-4939-1435-7_15. PubMed PMID: 25173170.
40. de Castro RO, Previato L, Goitea V, Felberg A, Guiraldelli MF, Filiberti A, et al. The Chromatin-remodeling Subunit Baf200 Promotes Homology-directed DNA Repair and Regulates Distinct Chromatin-remodeling Complexes. J Biol Chem. 2017. doi: 10.1074/jbc.M117.778183. PubMed PMID: 28381560.
41. Schubert M, Lindgreen S, Orlando L. AdapterRemoval v2: rapid adapter trimming, identification, and read merging. BMC Res Notes. 2016;9:88. Epub 2016/02/13. doi:

10.1186/s13104-016-1900-2. PubMed PMID: 26868221; PubMed Central PMCID: PMCPMC4751634.
42. Lindgreen S. AdapterRemoval: easy cleaning of next-generation sequencing reads. BMC Res Notes. 2012;5:337. Epub 2012/07/04. doi: 10.1186/1756-0500-5-337. PubMed PMID: 22748135; PubMed Central PMCID: PMCPMC3532080.
43. Li H, Durbin R. Fast and accurate short read alignment with Burrows-Wheeler transform. Bioinformatics. 2009;25(14):1754-60. Epub 2009/05/20. doi: 10.1093/bioinformatics/btp324. PubMed PMID: 19451168; PubMed Central PMCID: PMCPMC2705234.
44. Li H, Durbin R. Fast and accurate long-read alignment with Burrows-Wheeler transform. Bioinformatics. 2010;26(5):589-95. Epub 2010/01/19. doi: 10.1093/bioinformatics/btp698. PubMed PMID: 20080505; PubMed Central PMCID: PMCPMC2828108.
45. Li H, Handsaker B, Wysoker A, Fennell T, Ruan J, Homer N, et al. The Sequence Alignment/Map format and SAMtools. Bioinformatics. 2009;25(16):2078-9. Epub 2009/06/10. doi: 10.1093/bioinformatics/btp352. PubMed PMID: 19505943; PubMed Central PMCID: PMCPMC2723002.
46. Ewels P, Magnusson M, Lundin S, Kaller M. MultiQC: summarize analysis results for multiple tools and samples in a single report. Bioinformatics. 2016;32(19):3047-8. Epub 2016/06/18. doi: 10.1093/bioinformatics/btw354. PubMed PMID: 27312411; PubMed Central PMCID: PMCPMC5039924.
47. Landt SG, Marinov GK, Kundaje A, Kheradpour P, Pauli F, Batzoglou S, et al. ChIP-seq guidelines and practices of the ENCODE and modENCODE consortia. Genome Res. 2012;22(9):1813-31. doi: 10.1101/gr.136184.111. PubMed PMID: 22955991; PubMed Central PMCID: PMCPMC3431496.
48. Kharchenko PV, Tolstorukov MY, Park PJ. Design and analysis of ChIP-seq experiments for DNA-binding proteins. Nat Biotechnol. 2008;26(12):1351-9. Epub 2008/11/26. doi: 10.1038/nbt.1508. PubMed PMID: 19029915; PubMed Central PMCID: PMCPMC2597701.
49. Robinson JT, Thorvaldsdottir H, Winckler W, Guttman M, Lander ES, Getz G, et al. Integrative genomics viewer. Nat Biotechnol. 2011;29(1):24-6. Epub 2011/01/12. doi: 10.1038/nbt.1754. PubMed PMID: 21221095; PubMed Central PMCID: PMCPMC3346182.
50. Thorvaldsdottir H, Robinson JT, Mesirov JP. Integrative Genomics Viewer (IGV): high-performance genomics data visualization and exploration. Brief Bioinform. 2013;14(2):178-92. Epub 2012/04/21. doi: 10.1093/bib/bbs017. PubMed PMID: 22517427; PubMed Central PMCID: PMCPMC3603213.
51. Zhang Y, Liu T, Meyer CA, Eeckhoute J, Johnson DS, Bernstein BE, et al. Model-based analysis of ChIP-Seq (MACS). Genome Biol. 2008;9(9):R137. Epub 2008/09/19. doi: 10.1186/gb-2008-9-9-r137. PubMed PMID: 18798982; PubMed Central PMCID: PMCPMC2592715.
52. Quinlan AR, Hall IM. BEDTools: a flexible suite of utilities for comparing genomic features. Bioinformatics. 2010;26(6):841-2. Epub 2010/01/30. doi: 10.1093/bioinformatics/btq033. PubMed PMID: 20110278; PubMed Central PMCID: PMCPMC2832824.
53. Yu G, Wang LG, He QY. ChIPseeker: an R/Bioconductor package for ChIP peak annotation, comparison and visualization. Bioinformatics. 2015;31(14):2382-3. Epub 2015/03/15. doi: 10.1093/bioinformatics/btv145. PubMed PMID: 25765347.

Figure Legends

Figure 1. CHD4 expression and formation of different NURD complexes during gametogenesis. (A) Expression of *Chd4* monitored by immunofluorescence in testis sections of 14dpp and 2 months (adult) old mouse using two distinct antibodies against CHD4, a rabbit polyclonal anti-CHD4 and anti-PLZF (top panel) and mouse monoclonal anti-CHD4 and anti-SOX9 (bottom panel). Arrows indicate examples of CHD4 positive spermatogonia (PLZF) or Sertoli (SOX9) cells. Cells within the punctuated line are pachytene spematocytes. **(B)** Spermatocyte chromosome spread obtained from two months old mouse testes immunostained with antibodies specific for CHD4, SYCP3, and γH2AX (the last two markers of primary spermatocytes). Arrows indicate CHD4 signal at the X-Y pseudoautosomal region. These are examples of images obtained from 3 different mice. **(C)** Western blot analysis of different NURD components in fractions of cells enriched in Sertoli cells (SOX9 positive), undifferentiated (THY1.2+) (PLZF positive) and differentiating spermatogonia (c-KIT+) (STRA8 positive), pachytene primary spermatocytes (SYCP3 positive). Lamin B (Lam B) and α-tubulin (Tub) were used as loading standards. The scheme represents the composition of a canonical NURD complex. **(D)** CHD4-participating NURD complexes in spermatogonia and Sertoli cells assessed by coimmunoprecipitation with anti-CHD4 as a bait. Non-specific IgG was used as a bait control. Experiments were repeated twice, and the star marks an unspecific reactive band.

Figure 2. *Chd4* and *Chd3* gene targeting design and testis developmental defects in *Chd4* mutant mice. (A and B) Testis specific Cre knockout strategy for deletion of *Chd4* and *Chd3*. See description Materials and Methods. **(C)** The panel shows expected time of

expression for Ddx4-Cre and Spo11-Cre used in this study. **(D)** (top and middle panels) *Chd4* and *Chd3* transcription levels expression were measured in Ddx4-CHD3$^{-/-}$ total testis or Spo11-CHD4$^{-/-}$ and compared to wild type littermates (two months old mice, n=3). The lower panel show Chd4 transcription level in isolated spermatogonia obtained from 7dpp Ddx4-CHD4$^{-/-}$ and control wild type litter mate mice (mice, biological replicate n=3). **(E)** H&E stained paraffin testis sections of wild type, Ddx4-*Chd4*$^{-/-}$, Spo11-*Chd4*$^{-/-}$, and Ddx4-*Chd3*$^{-/-}$ mice. Quantification of testis weight for wild type and homozygous knockout mice is also shown. Images and testis weigh measurements were obtained from at least three mice.

Figure 3. Ddx4-*Chd4*$^{-/-}$ mice show profound defects in gametogenesis. (A) H&E-stained histological sections of wild type and Ddx4-*Chd4*$^{-/-}$ testis. Stars mark seminiferous tubules with absent germ cells. Note unchanged number and morphology of Sertoli cells (indicated by green arrows). **(B)** Histological sections of wild type and Ddx4-*Chd4*$^{-/-}$ testis showing seminiferous tubules immunolabeled with SOX9 (a marker of Sertoli cells) and TRA98 (to mark germ cells). P, pachytene cells; Se, Sertoli cells; Rs, rounded spermatids. **(C)** H&E-stained histological sections of wild type and Ddx4-*Chd4*$^{-/-}$ ovaries. F, follicles and CL, corpora lutea.

Figure 4. Spermatogonia cell survival requires CHD4. (A) Histological sections of wild type and Ddx4-*Chd4*$^{-/-}$ testis cord from 9 days old mice stained with H&E (a and b), immunostained with TRA98 antibodies (marking germ cells, c and d), and Hematoxylin and immunostained with STRA8 antibodies (marking differentiating spermatogonia) (e and f). Arrows mark type of cells present in wild type but reduced in number or absent in the mutant. Experiments were done in at least three different mice showing similar results. **(B)** Immunostaining of sections of developing testis reveals severe loss of germ cells

(TRA98) in *Chd4*$^{-/-}$ testis cords. **(C)** Quantitation of number of cell positive for TRA98 and PLZF shown in B and SOX9. 3dpp testes TRA98, wild type (mean ± standard deviation) 4.1 ± 1.7, n=43; *Chd4*$^{-/-}$ *2.7* ± 1.4, n=60, P<0.0001, t test). *4dpp testis* (PLZF, wild type, 9.9 ± 4.1, n=47; *Chd4*$^{-/-}$ 2.2 ± 1.4, n=56, P<0.0001, t test. TRA98, wild type 12.6 ± 5.3, n=35; *Chd4*$^{-/-}$ *3.0* ± 1.9, n=37, P<0.0001, t test). *7dpp testes* (PLZF, wild type, 14.6 ± 5.0, n=28; *Chd4*$^{-/-}$ 3.4 ± 2.4, n=45, P<0.0001, t test. TRA98, wild type 19.6 ± 5.9, n=48; *Chd4*$^{-/-}$ *3.0* ± 2.1, n=24, P<0.0001, t test). Experiments were done in three different mice showing similar results. **(D)** Higher cell death in *Chd4*$^{-/-}$ knockout testes than in wild type controls at four days post-partum. Apoptotic cells were visualized by staining for TUNEL in three mice of each genotype. The percentage of apoptotic cells was counted only in the tubule cross-sections that contained apoptotic cells and was normalized to total number of germ cells. 19.05 ± 11.17, n=468 (mean ± SD, n= number of seminiferous tubules counted) wild type and 38.25 ± 13.72 *Chd4*$^{-/-}$ knockout, n=344; P<0.0001 (two-tailed Student t test). Experiments were done in three different mice. The arrow indicate apoptotic cells and arrowhead non-apoptotic germ cells.

Figure 5. CHD4 genome-wide chromatin binding profile and analysis. (A) Heatmaps showing CHD4 occupancy centered in transcription start site (TSS) for all genes (left panel) and in between TSS and transcription end site (TES) clustered according to the distribution of the signal (right panel). **(B)** Aggregate profiles corresponding to CHD4 signal between TSS and TES according to the distribution of the ChIP-seq signal. **(C)** Examples of CHD4 occupancy at or near a gene promoter assessed by ChIP-seq. **(D)** Pie chart depicting genomic features associated with CHD4 peaks. **(E)** Gene ontology analysis of genes associated to CHD4 ChIP-seq signals**. (F)** Selected genes with associated CHD4 binding sites corresponding to possible function and gene functional analysis.

Figure 6. Effect of Chd4 deletion in Dmrt1 and Plzf expression. (A) CHD4 occupancy at Dmrt1 gene promoter assessed by ChIP-seq. (**B**) Histological sections of wild type and Ddx4-*Chd4*$^{-/-}$ testis from 1, 4, and 7 dpp mice stained with CHD4 and DMRT1 antibodies. Arrows indicate examples of CHD4 positive spermatogonia (Wt) or CHD4 reduced staining in Ddx4-*Chd4*$^{-/-}$ spermatogonia and the correspondent cell stained for DMRT1. **(C)** Quantitation of fluorescence intensity of DMRT1 expression on spermatogonia is shown for wild type (Wt) and Ddx4-*Chd4*$^{-/-}$ knockout at ages of 1dpp (Wt = 82.17 ± 22.02, n=272; and KO = 37.20 ± 10.01, n=287, P<0.0001, Student t test) and 4dpp (Wt = 71.09 ± 20.93, n=242; and KO = 43.47 ± 14.88, n=198, P<0.0001, Student t test). Values represent the median fluorescence intensity ± standard deviation, n = total number of cells analyzed from 2 biological replicates using two different mice. (**D**) Dmrt1 gene expression in Chd4 knockout and wild type assessed by *Chd4* by RT-qPCR (Wt = 1.07 ± 0.16; and Ddx4-*Chd4*$^{-/-}$ = 0.24 ± 0.21, n=3, P=0.019, paired Student t test). (**E**) Histological sections of wild type and Ddx4-*Chd4*$^{-/-}$ testis from 1, 4, and 7dpp mice stained with antibodies against PLZF. **(F)** Quantitation of fluorescence intensity of PLZF expression on spermatogonia is shown for wild type and Ddx4-*Chd4*$^{-/-}$ knockout at ages of 1dpp (wt = 17.94 ± 4.10, n=300; and Ddx4-*Chd4*$^{-/-}$ = 10.89 ± 4.07, n=339, P<0.0001, Student t test) and 4dpp (Wt = 17.78 ± 4.70, n=282; and Ddx4-*Chd4*$^{-/-}$ = 9.11 ± 3.75, n=230, P<0.0001, Student t test). Values represent the median fluorescence intensity ± standard deviation, n = total number of cells analyzed from 2 biological replicates using two different mice. **(G)** Diagram representing CHD4, DMRT1, and PLZF relationship in spermatogonia stem cell maintenance.

Figure 7. Diagram summarizing the proposed functions of CHD4 during early gametogenesis and the effect of *Chd4* deletion in testis development. Undiff Spg: undifferentiated spermatogonia, Diff Spg: differentiating spermatogonia, PI Spc: Pre-

leptotene spermatocyte, Primary Spc: primary spermatocytes (leptotene-diplotene), Sec Spc: secondary spermatocyte.

Figure 1

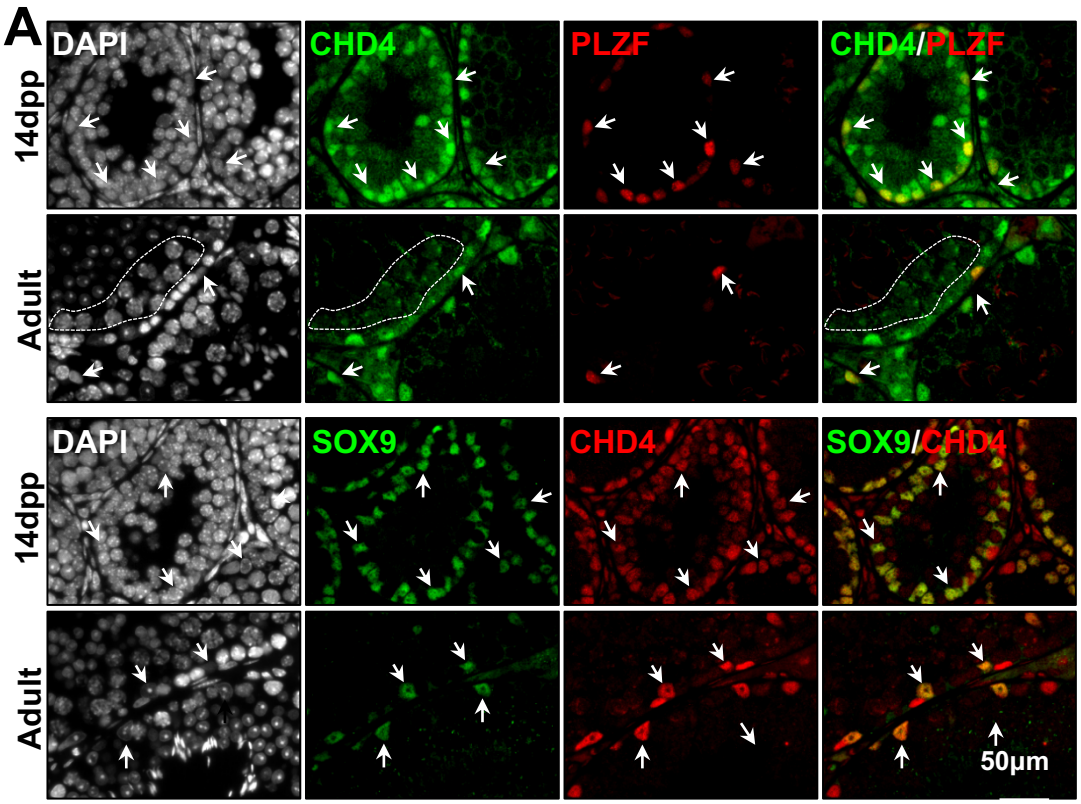
A
DAPI
CHD4
PLZF
CHD4/PLZF
14dpp
Adult
DAPI
SOX9
CHD4
SOX9/CHD4
14dpp
Adult
50μm

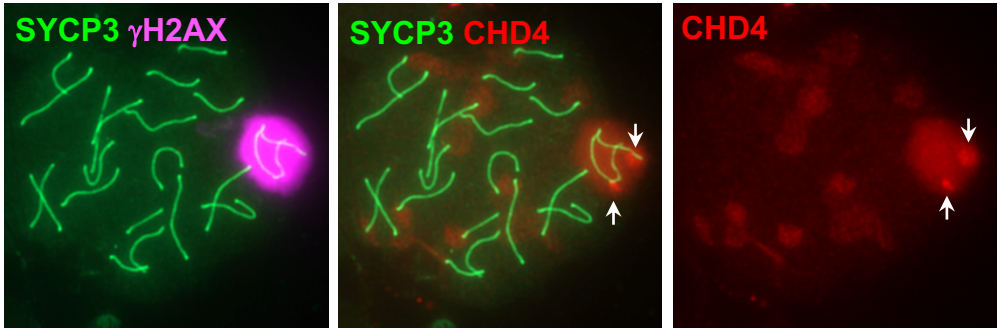
B
SYCP3 γH2AX
SYCP3 CHD4
CHD4

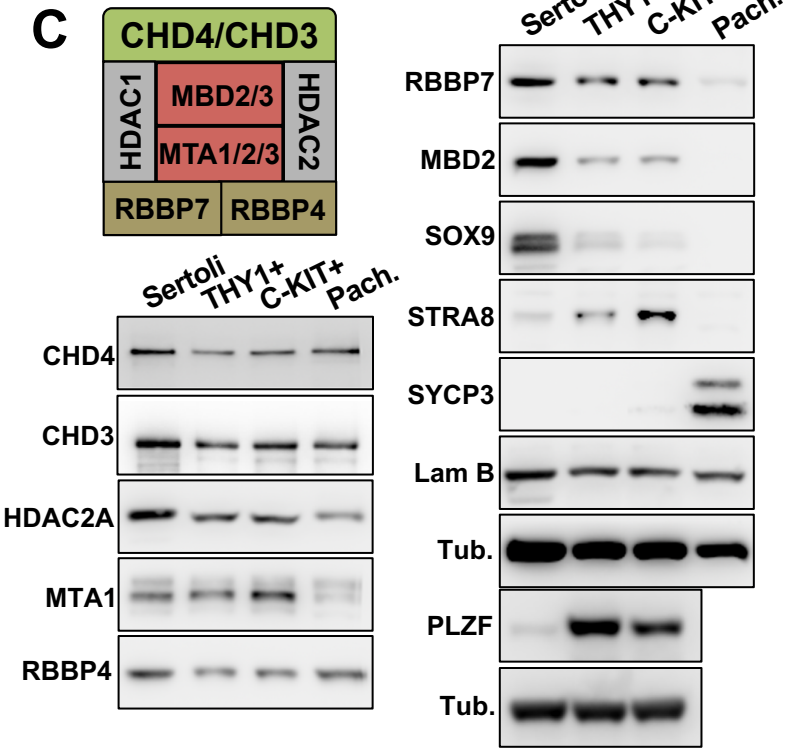
C
CHD4/CHD3
HDAC1
MBD2/3
HDAC2
MTA1/2/3
RBBP7
RBBP4
Sertoli
THY1+
C-KIT+
Pach.
CHD4
CHD3
HDAC2A
MTA1
RBBP4
RBBP7
MBD2
SOX9
STRA8
SYCP3
Lam B
Tub.
PLZF
Tub.

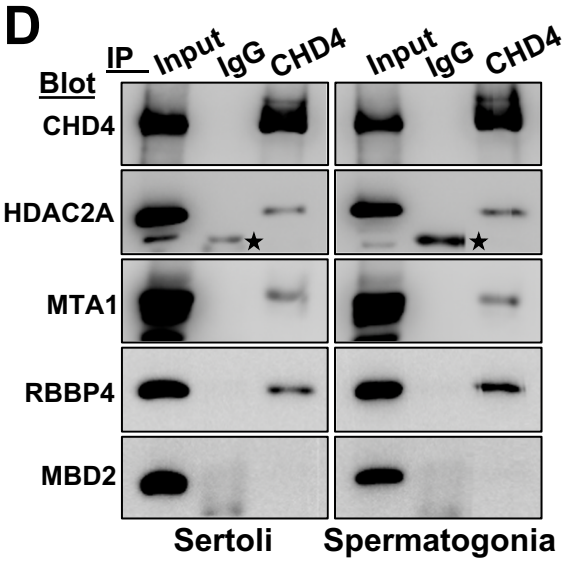
D
IP
Input
IgG
CHD4
Input
IgG
CHD4
Blot
CHD4
HDAC2A
MTA1
RBBP4
MBD2
Sertoli
Spermatogonia

Figure 2

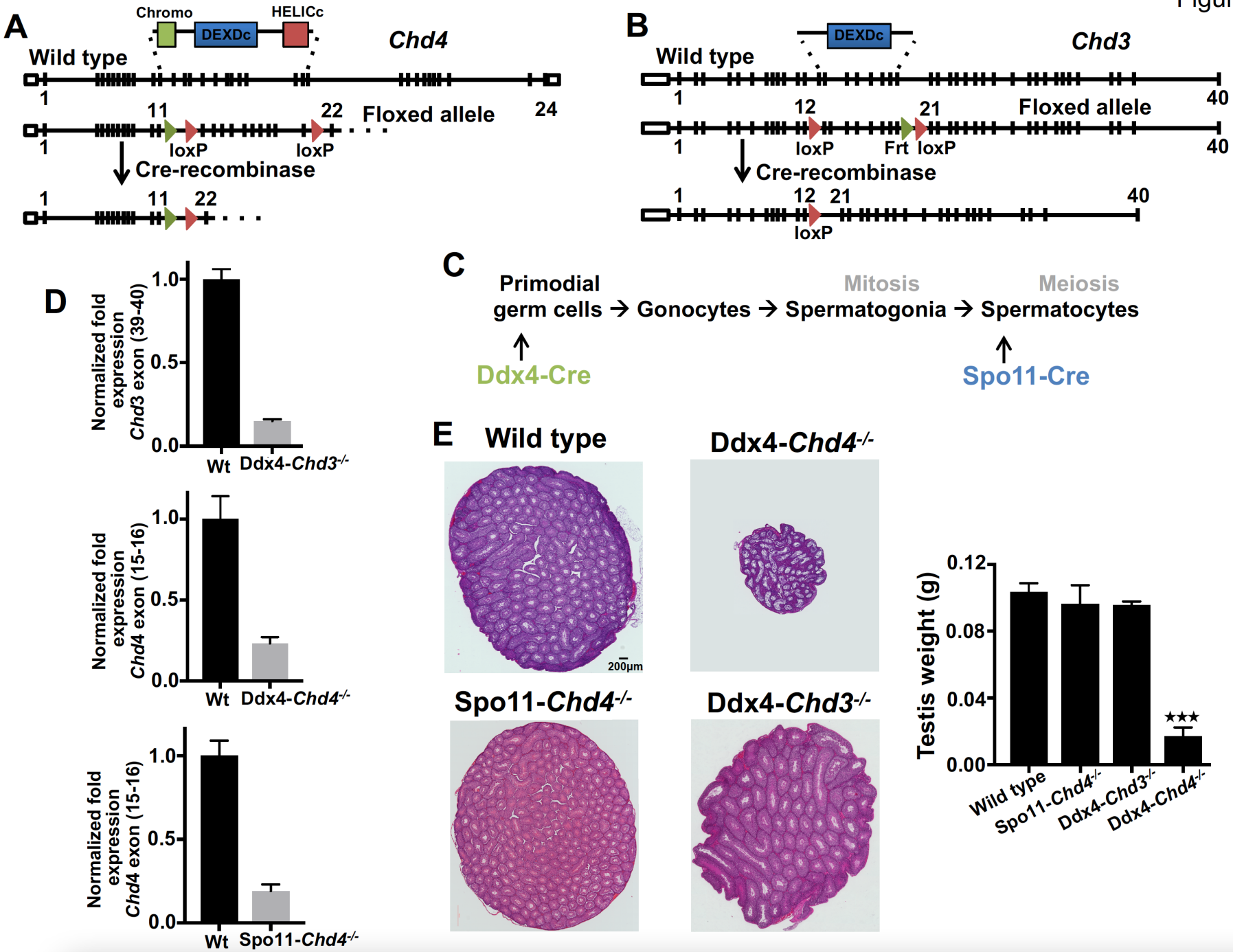
A
Chromo
HELICc
DEXDc
Chd4
Wild type
1
11
22
24
Floxed allele
loxP
loxP
Cre-recombinase
B
DEXDc
Chd3
Wild type
1
12
21
40
Floxed allele
loxP
Frt
loxP
Cre-recombinase
C
Primodial germ cells → Gonocytes → Spermatogonia → Spermatocytes
Mitosis
Meiosis
Ddx4-Cre
Spo11-Cre
D
Normalized fold expression Chd3 exon (39-40)
Wt
Ddx4-Chd3-/-
Normalized fold expression Chd4 exon (15-16)
Wt
Ddx4-Chd4-/-
Normalized fold expression Chd4 exon (15-16)
Wt
Spo11-Chd4-/-
E
Wild type
Ddx4-Chd4-/-
200µm
Spo11-Chd4-/-
Ddx4-Chd3-/-
Testis weight (g)
0.12
0.08
0.04
0.00
★★★
Wild type
Spo11-Chd4-/-
Ddx4-Chd3-/-
Ddx4-Chd4-/-

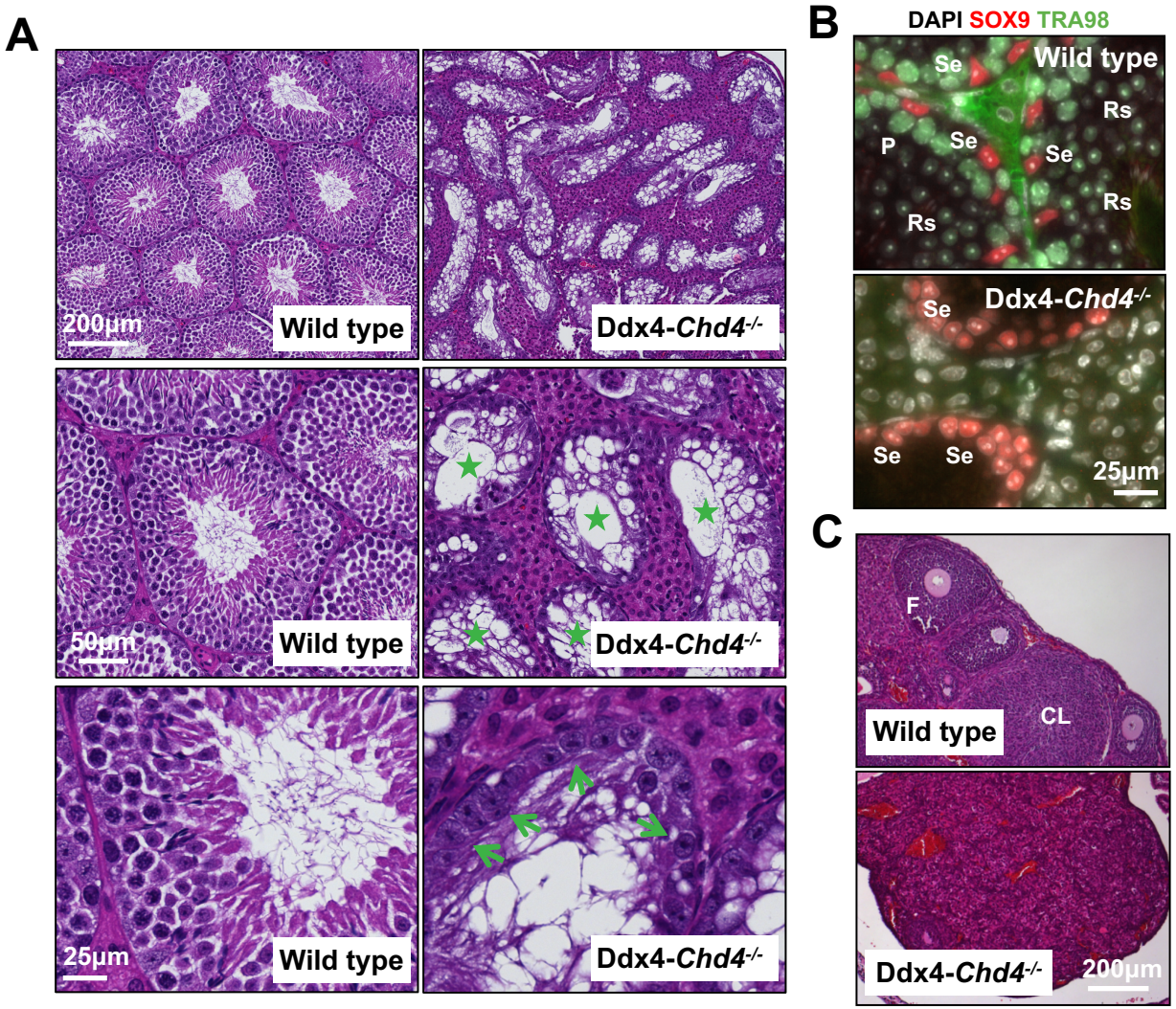
A
200μm
Wild type
Ddx4-Chd4-/-
50μm
Wild type
Ddx4-Chd4-/-
25μm
Wild type
Ddx4-Chd4-/-
B
DAPI SOX9 TRA98
Se
Wild type
Rs
P
Se
Se
Rs
Rs
Se
Ddx4-Chd4-/-
Se
Se
25μm
C
F
CL
Wild type
Ddx4-Chd4-/-
200μm

Figure 4

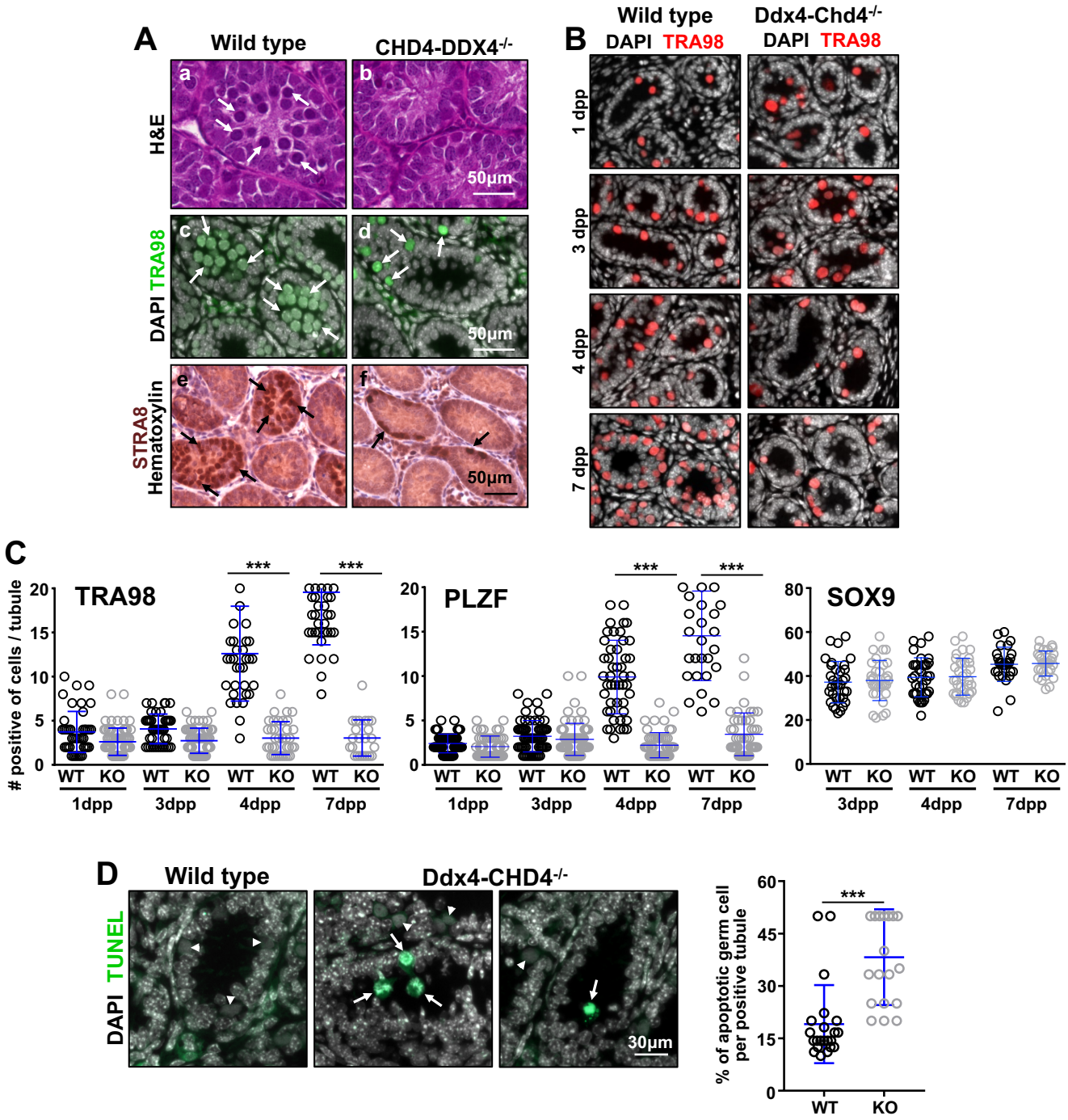
A
Wild type
CHD4-DDX4-/-
H&E
DAPI TRA98
STRA8
Hematoxylin
a
b
c
d
e
f
50µm
B
Wild type
Ddx4-Chd4-/-
DAPI TRA98
1 dpp
3 dpp
4 dpp
7 dpp
C
TRA98
PLZF
SOX9
positive of cells / tubule
***
WT KO
1dpp
3dpp
4dpp
7dpp
D
Wild type
Ddx4-CHD4-/-
DAPI TUNEL
30µm
% of apoptotic germ cell per positive tubule
WT
KO

Figure 5

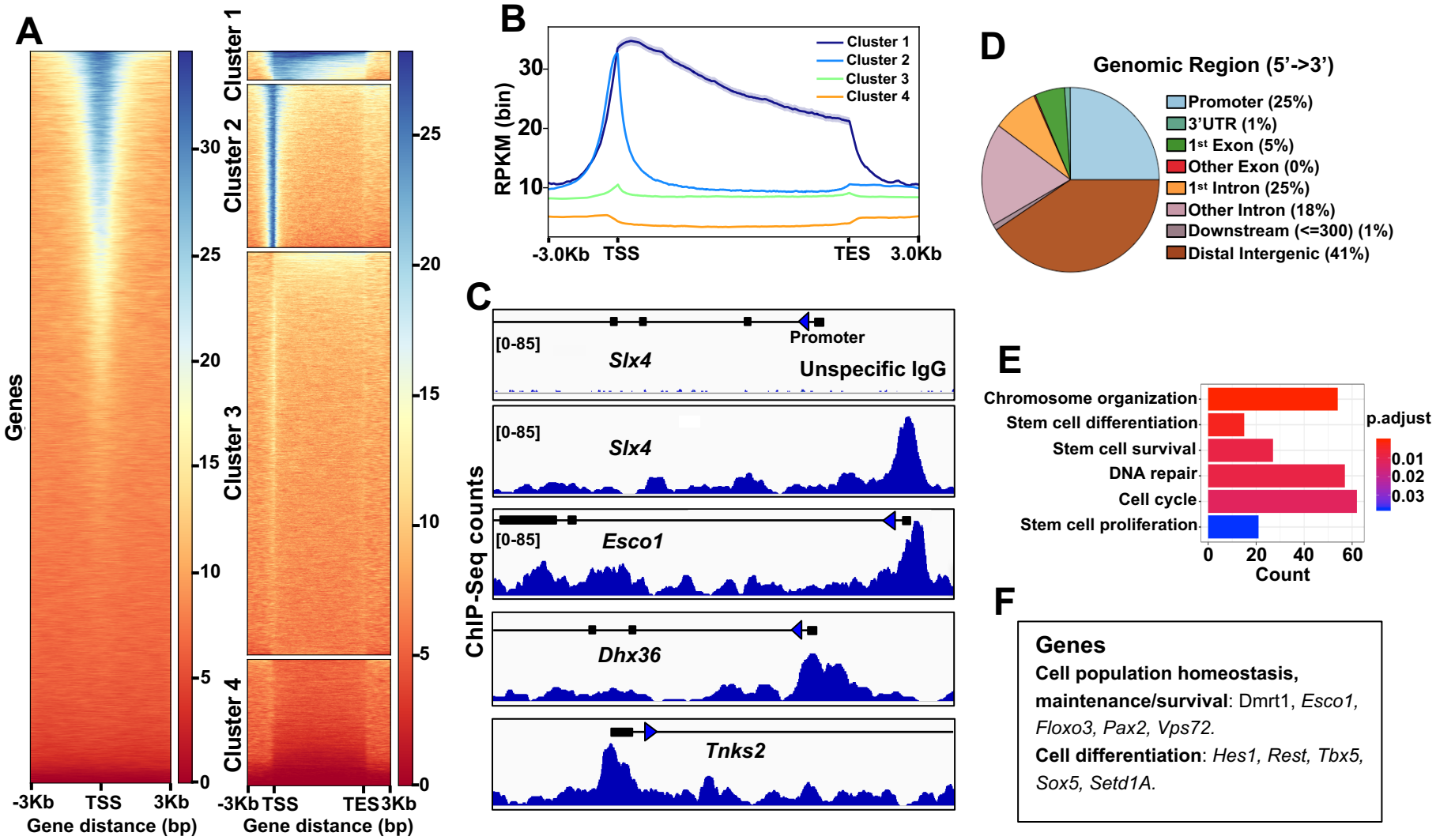
A
Genes
Cluster 1
Cluster 2
Cluster 3
Cluster 4
-3Kb TSS 3Kb
Gene distance (bp)
-3Kb TSS TES 3Kb
Gene distance (bp)
B
RPKM (bin)
Cluster 1
Cluster 2
Cluster 3
Cluster 4
-3.0Kb TSS TES 3.0Kb
C
ChIP-Seq counts
[0-85]
Slx4
Promoter
Unspecific IgG
Esco1
Dhx36
Tnks2
D
Genomic Region (5'->3')
Promoter (25%)
3'UTR (1%)
1st Exon (5%)
Other Exon (0%)
1st Intron (25%)
Other Intron (18%)
Downstream (<=300) (1%)
Distal Intergenic (41%)
E
Chromosome organization
Stem cell differentiation
Stem cell survival
DNA repair
Cell cycle
Stem cell proliferation
p.adjust
0.01
0.02
0.03
Count
F
Genes
Cell population homeostasis, maintenance/survival: Dmrt1, Esco1, Floxo3, Pax2, Vps72.
Cell differentiation: Hes1, Rest, Tbx5, Sox5, Setd1A.

Figure 6

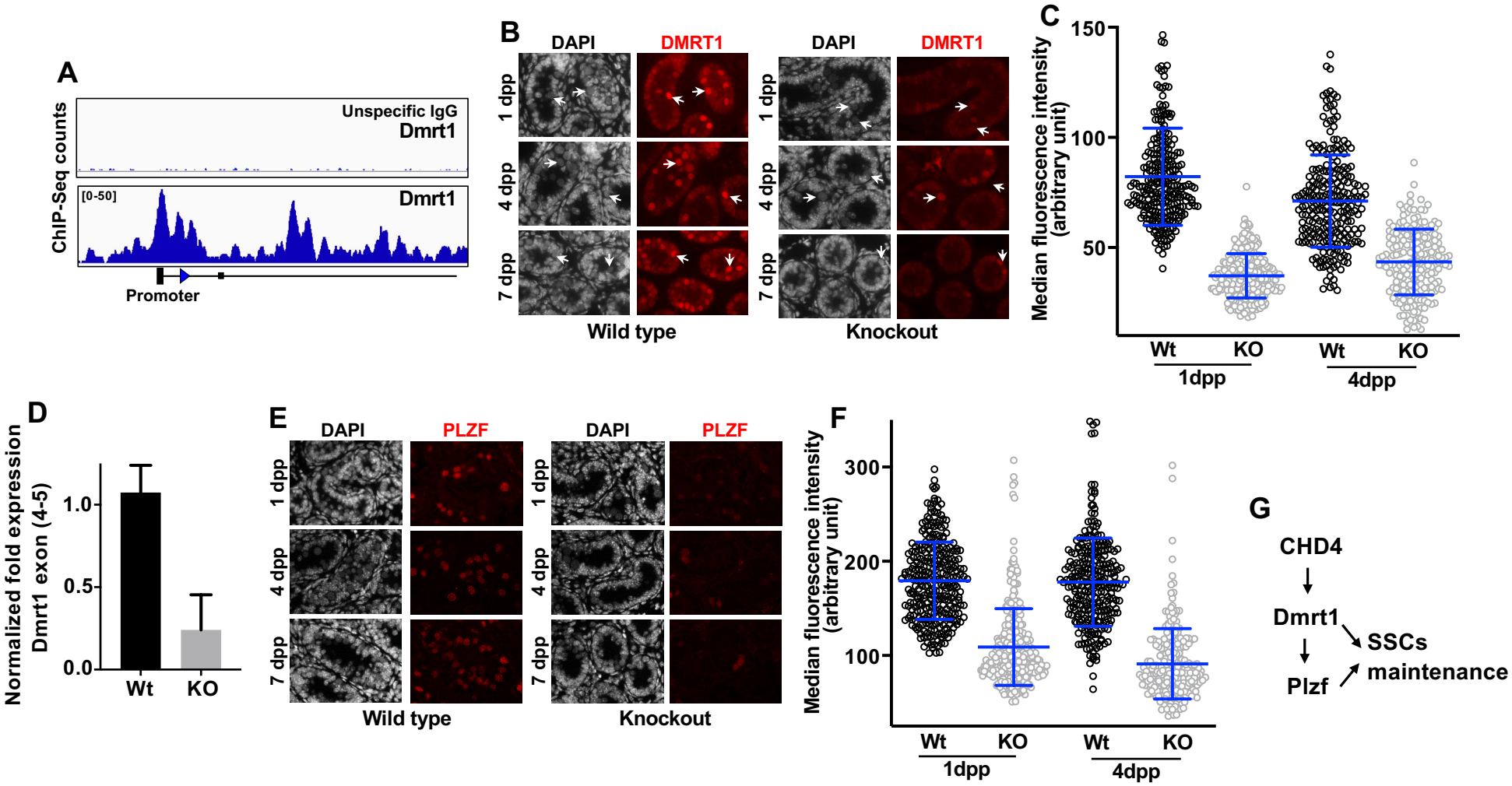
A
ChIP-Seq counts
Unspecific IgG
Dmrt1
[0-50]
Dmrt1
Promoter
B
DAPI
DMRT1
1 dpp
4 dpp
7 dpp
Wild type
Knockout
C
Median fluorescence intensity (arbitrary unit)
150
100
50
Wt
KO
1dpp
4dpp
D
Normalized fold expression Dmrt1 exon (4-5)
1.0
0.5
0.0
Wt
KO
E
PLZF
F
300
200
100
G
CHD4
Dmrt1
Plzf
SSCs maintenance

Figure 7

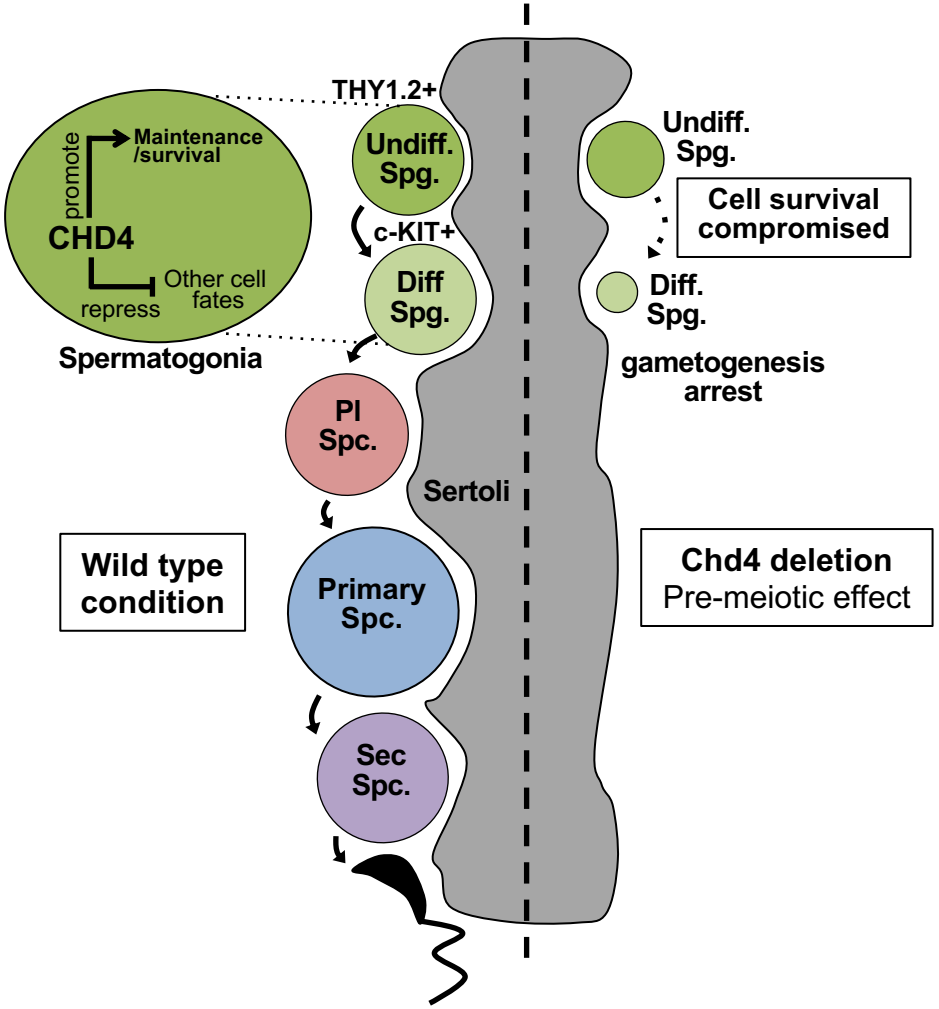
THY1.2+
Maintenance /survival
promote
CHD4
Other cell fates
repress
Spermatogonia
Undiff. Spg.
c-KIT+
Diff Spg.
Pl Spc.
Primary Spc.
Sec Spc.
Sertoli
Wild type condition
Undiff. Spg.
Cell survival compromised
Diff. Spg.
gametogenesis arrest
Chd4 deletion
Pre-meiotic effect